Let bone and muscle talk together: a study of real and virtual dissection and its implications for femoral musculoskeletal structure of chimpanzees

Morimoto, Naoki ; Suwa, Gen ; Nishimura, Takeshi ; Ponce de León, Marcia S ; Zollikofer, Christoph P E ; Lovejoy, C Owen ; Nakatsukasa, Masato

Abstract: Proximal femoral morphology and associated musculature are of special relevance to the understanding of hominoid locomotor systems. Knowledge of bone-muscle correspondence in extant hominoids forms an important comparative basis for inferring structure-function relationships in fossil hominids. However, there is still a lack of consensus on the correspondence between muscle attachment sites and surface morphology of the proximal femoral diaphysis in chimpanzees. Two alternative observations have been proposed regarding the attachment site positions of gluteus maximus (GM) and vastus lateralis (VL) relative to two prominent surface features of the proximal femoral diaphysis, the lateral spiral pilaster and the inferolateral fossa. Here, we use a combination of virtual and physical dissection in an attempt to identify the exact correspondence between muscle attachment sites and osteological features in two specimens of Pan troglodytes verus. The results show that the insertion of the GM tendon is consistently inferolateral to the lateral spiral pilaster, and that a part of the inferolateral fossa consistently forms the attachment site of the VL muscular fibers. While overall musculoskeletal features are similar in the two specimens examined in this study, GM and VL exhibit different degrees of segregation at the level of the inferolateral fossa. One specimen exhibited tendinous GM fibers penetrating the posteromedial part of VL, with both GM and VL inserting at the inferolateral fossa. In the other specimen, GM and VL were separated by a lateral intermuscular septum, which inserted into the inferolateral fossa. Variation of proximal femoral muscle attachments in chimpanzees is thus greater than previously thought. Our results indicate that a conspicuous osteological feature such as the inferolateral fossa does not necessarily correspond to the attachment site of a single muscle, but could serve as a boundary region between two muscles. Caution is thus warranted when interpreting the surface topography of muscle attachment sites and inferring locomotor functions.

DOI: https://doi.org/10.1111/joa.12270

Let bone and muscle talk together: a study of real and virtual dissection and its implications for femoral musculoskeletal structure of chimpanzees

Naoki Morimoto[1], Gen Suwa[2], Takeshi Nishimura[3], Marcia S. Ponce de León[4], Christoph P.E. Zollikofer[4], C.Owen Lovejoy[5], Masato Nakatsukasa[1]

[1] *Laboratory of Physical Anthropology, Graduate School of Science, Kyoto University, Japan*
[2] *The University Museum, The University of Tokyo, Hongo, Bunkyo-ku, Tokyo, Japan*
[3] *Primate Research Institute, Kyoto University, Inuyama, Japan*
[4] *Anthropological Institute, University of Zurich, Switzerland*
[5] *Department of Anthropology, School of Biomedical Sciences, Kent State University, Ohio, USA*

Abstract

Proximal femoral morphology and associated musculature are of special relevance to the understanding of hominoid locomotor systems. Knowledge of bone-muscle correspondence in extant hominoids forms an important comparative basis in inferring structure-function relationships in fossil hominids. However, there is still a lack of consensus on the correspondence between muscle attachment sites and surface morphology of the proximal femoral diaphysis in chimpanzees. Two alternative observations have been proposed regarding the attachment site positions of *gluteus maximus* (GM) and *vastus lateralis* (VL) relative to two prominent surface features of the proximal femoral diaphysis, the lateral spiral pilaster and the inferolateral fossa. Here, we use a combination of virtual and physical dissection in an attempt to identify the exact correspondence between muscle attachment sites and osteological features in two specimens of *Pan troglodytes verus*. The results show that the insertion of the GM tendon is consistently inferolateral to the lateral spiral pilaster, and that a part of the inferolateral fossa consistently forms the attachment site of the VL muscular fibers. While overall musculoskeletal features are similar in the two specimens examined in this study, GM and VL exhibit different degrees of segregation at the level of the inferolateral fossa. One specimen exhibited tendinous GM fibers penetrating the posteromedial part of VL, with both GM and VL inserting at the inferolateral fossa. In the other specimen, GM and VL were separated by a lateral intermuscular septum, which inserted into the inferolateral fossa. Variation of proximal femoral muscle attachments in chimpanzees is thus greater than previously thought. Our results indicate that a conspicuous osteological feature such as the inferolateral fossa does not necessarily correspond to the attachment site of a single muscle, but could serve as a boundary region between two muscles. Caution is thus warranted when interpreting the surface topography of muscle attachment sites and inferring locomotor functions.

Key words: comparative anatomy; great ape; femoropelvic musculature; *gluteus maximus*; *Pan troglodytes*

Introduction

Among living primates, bipedal locomotion with upright posture and extended hips and knees is specific to humans and contrasts with quadrupedal and suspensory locomotion of great apes. Evolution of locomotor behaviors in humans and great apes is thought to be accompanied by reorganization of femoropelvic musculoskeletal structure (Stern, 1972, Lovejoy et al., 2002). Among the locomotor muscles, *gluteus maximus* (GM) often attracts special interest because it is an important component of hind limb-mediated primate locomotor activities. Various studies have documented taxon-specific features of this muscle in primates (Beddard, 1893, Champneys, 1871, Crass, 1952, Hepburn, 1892, Primrose, 1898, Raven, 1950, Sigmon, 1974, Stern, 1972, Uhlmann, 1968). Humans are distinct from great apes in various aspects of GM structure. In humans, the GM is larger relative to body mass than in great apes (thus the term "*maximus*") (Thorpe et al., 1999, Lieberman et al., 2006, Voronov, 2003). Likewise, structure of the vastus muscles, a substantial knee extensor, is different between humans and great apes. Vastus muscles of modern humans are large relative to adductor and hamstring muscles (Lovejoy et al., 2002). In great apes, the GM originates from the sacro-iliac region, coccyx, sacro-tuberous ligament (except in orangutans), and ischial tuberosity. The great ape GM inserts into the *vastus lateralis* (VL) aponeurosis (a part of the iliotibial tract (IT)), and along the lateral side of the femoral diaphysis (Stern, 1972, Uhlmann, 1968, Primrose, 1898, Sigmon, 1974). In contrast, the human GM does not have an ischial origin, and its insertion is confined to the proximal femoral shaft and associated connective tissues. Furthermore, in humans, the GM faces more posteriorly and serves as an extensor of the hip joint, whereas, in great apes, the GM faces more laterally and serves more as an abductor (Lovejoy et al., 2002). The human GM is thus unique in terms of its relative size, position, orientation, and function.

The human-specific features of the GM are thought to be related to stabilizing the hip joint during bipedal locomotion (Stern and Susman, 1981, Lovejoy, 2005) and in other activities such as throwing (Marzke et al., 1988). Perhaps its most important role is its capacity to resist anterior-ward trunk flexion that would otherwise occur at heel strike during running (Lovejoy, 2005), as the human GM is recruited during running rather than in walking. It has been suggested that its morphology represents an adaptation to long-distance running (Bramble and Lieberman, 2004, Lieberman et al., 2006), but this hypothesis is challenged by a recent experimental study, which showed that locomotor muscles are not optimized for a specific locomotor mode but are sub-optimized to a variety of separate locomotor behaviors (Carrier et al., 2011).

Establishing anatomical correspondences between soft- and hard-tissue structures in the extant human and great ape musculoskeletal systems is critical to the understanding of form-function relationships in fossil hominids (humans and their extinct relatives on the human side of the phylogenetic split with chimpanzees from the common ancestor). Various studies have shown that the surface morphologies of the human and great ape proximal femoral diaphysis are closely linked to the topography (attachment and orientation patterns) of GM and associated muscles (Lovejoy et al., 2002, Sigmon, 1974, Raven, 1950, Swindler and Wood, 1982). The proximal femur is thus a key region in reconstructing femoropelvic muscle topographies, and in inferring fossil hominid locomotor behaviors (Pickford et al., 2002, Lovejoy et al., 2002, Lovejoy et al., 2009b). However, detailed comparative information of extant humans and great apes is still relatively scarce, in part because it has proven difficult to obtain muscular and skeletal data from one and the same individual. Most classical studies combine soft and hard tissue data of different specimens/samples (soft tissue data from dissections, hard tissue data from osteological collections) (e.g., Swindler and Wood, 1982, Sigmon, 1974, Uhlmann, 1968). Musculoskeletal correspondence is then established, not by observing muscle attachments and bone in the same individual, but across individuals. Therefore, significant details of intraspecific variation of muscle attachment patterns may be lost. Recently, CT-based virtual dissection (virtopsy) has been proposed as an alternative new method, since this technique permits non-invasive acquisition of hard and soft tissue data from one and the same individual (Morimoto et al., 2011b, Thali et al., 2009, Thali et al., 2007). However, virtopsy has its own limitations. For example, it is often difficult to discriminate between areas of muscular insertion, and areas of mere musculoskeletal contact (adjacency).

As a consequence, the details of bone-muscle correspondence in the chimpanzee proximal femur remain unclear (especially regarding muscular and tendinous fibers), and alternative views exist on how the surface morphologies of the femoral diaphysis reflect muscle attachment sites (Lovejoy et al., 2002; Suwa et al., 2012 versus Morimoto et al., 2011b; details are provided in Fig. 1 and the next section). To resolve these issues, we conducted combined virtual and physical dissections of two *Pan troglodytes verus* specimens. Here we present the results of this study, including new information on muscle-bone correspondences and interindividual musculoskeletal variation of the proximal femoral region of *Pan*, as well as new perspectives on the potential and limitations of virtual dissection of great ape cadavers.

The musculoskeletal topography of the proximal femur in chimpanzees

Osteological features. The proximal femoral diaphysis of chimpanzees exhibits a ridge, or superoinferiorly extending prominence, defined as the lateral spiral pilaster (LSP) (Lovejoy et al., 2002).

This prominence curves diagonally down along the diaphysis, changing its position from lateral to postero-lateral (Fig. 1A, B). In chimpanzees, the LSP delimits two rugose fossa-like depressions situated superomedially and inferolaterally (superomedial fossa [SMF] and inferolateral fossa [ILF]) to the LSP, respectively (Fig. 1A, B). There is considerable variation in the degree of development, shape, and the relative position of the LSP and adjacent fossae. For example, the morphology of LSP varies from a well-developed ridge to a rugose lipped structure, and the development of the ILF fossa varies from well-marked to weakly-expressed concavities (Morimoto et al., 2011a).

Soft-tissue features. In chimpanzees, the anterior part of GM inserts directly on the proximal femur by means of a well-developed tendon (Stern, 1972). This tendon is referred to as the ascending tendon (AT) "because its anterior fibers insert most distally, while the more posterior ones attach progressively higher on the femur" (cited from Stern, 1972; p. 318). On the other hand, the posterior part of the GM (in part) inserts distally to the *vastus lateralis* (VL) aponeurosis (Stern, 1972).

Bone-muscle correspondence. Fig. 1(C, D) summarizes the muscle attachment site patterns of the chimpanzee proximal femoral diaphysis, as proposed by Lovejoy et al. (Suwa et al., 2012, Lovejoy et al., 2002), and by Morimoto et al. (Morimoto et al., 2011b), respectively. Both Lovejoy et al. and Morimoto et al. identified the superomedial fossa (SMF) as an attachment site for the *adductor brevis/minimus* (see issues of adductor complexity discussed in Lovejoy et al., 2002). Lovejoy et al. proposed that ILF serves as an attachment site for the GM, but not for VL. Accordingly, the attachment site of GM is considered anterolateral to (or marginally on) LSP, while the attachment site of VL is considered anterior to ILF (Fig. 1C). The LSP was considered to occur between the AD and GM attachment areas. On the other hand, Morimoto et al. proposed that ILF serves as an attachment site of VL, while the attachment site of GM was considered posteromedial to LSP (Fig. 1D). The two different views on the topography of muscle attachment sites resulted in different views on the attachment site of the lateral intermuscular septum (LIM), which is the boundary structure between GM and VL. Lovejoy et al. proposed that LIM attaches at the anterior margin of ILF (Suwa et al., 2012), while Morimoto et al. proposed that LIM attaches typically on the LSP (and variants in the ILF). Furthermore, according to interpretations of Lovejoy et al., the VL aponeurosis, connected with the posterior part of GM should be situated at or anterior to the ILF margin. To the contrary, according to Morimoto et al., the VL aponeurosis should be situated on the LSP and/or at the ILF margin. To resolve the contradictions between these two propositions, we ask the following questions on femoral morphology and associated musculature in chimpanzees:

- Is the attachment site of the ascending tendon (AT) of *gluteus maximus* (GM) superomedial or inferolateral to the lateral spiral pilaster (LSP)?

- Is *vastus lateralis* (VL) attached on the *inferolateral fossa* (ILF)?
- Where does the lateral intermuscular septum (LIM) attach relative to the lateral spiral pilaster (LSP) and *inferolateral fossa* (ILF)?

Materials and methods

Sample

Two cadavers of adult (third molar erupted) female chimpanzees (*Pan troglodytes verus*) were obtained, one from the collections of Tobe Zoological Park/Tennoji Zoo, Japan (TZP/TZ; reference *id*: Sakura), and the other from the Higashiyama Zoo and Botanical Gardens, Japan (HZB; reference *id*: Rimi) (Table 1). The latter is currently housed in the Primate Research Institute of Kyoto University, Japan (KUPRI; reference *id*: PRISK-8828) (Table 1). Both specimens were CT-scanned prior to their physical dissection. The CT data are accessible at the Digital Morphology Museum of KUPRI (http://www.pri.kyoto-u.ac.jp/dmm/WebGallery/index.html; CT data *id*: PRICT-1022 [Sakura], PRICT-1023 [Rimi]). Sakura was a fresh cadaver during the CT scan and the first session of physical dissection. Its femoral and its surrounding area were then fixed with formalin prior to the second session of physical dissection. Rimi was fixed with formalin prior to the CT scan and the physical dissection.

Volumetric data acquisition and visualization

Both specimens were scanned using a 4-detector-array CT device (Toshiba, Asteion 4 Premium Edition) with the following parameters: beam collimation: 1.0 mm; slice increment: 0.2-0.4 mm; pitch: 0.75-0.875; image reconstruction kernel: standard and bone (FC03/FC30). This resulted in volume data sets with isotropic spatial resolution in the range of 0.4 to 0.5 mm. The software package Avizo 7.1 (VSG-Visualization Sciences Group) was used to visualize user-defined cross-sections of the musculoskeletal system, to extract the femoral surface, and to identify the spatial relationships between bone and muscle structures.

The surface topography of the femora was quantified with morphometric mapping methods (Morimoto et al., 2011a). The morphometric maps were then used to identify the relevant surface structures by C.P.E.Z. and M.S.P.d.L. without knowing the results of physical dissection. Morphometric mapping analyses were performed using MATLAB 8.2 (Math Works). Following dissection, the cadavers were skeletonized to allow direct observation of the bone surface topography.

Physical dissection

In both specimens, the right hindlimb was dissected using the same protocol. T.N. and M.N. performed the dissection, and N.M. and G.S. assisted the dissection. To expose the attachment sites of VL and GM at the regions of ILF and LSP, the vastus muscles and GM were partly detached from the femoral diaphysis. The muscular and tendinous fibers were then traced to identify the fiber orientation. Locations of attachment sites of tendinous structures on the femoral diaphysis were marked by cutmarks using a surgical knife, and were examined after skeletonization.

Results

Physical dissection

In both specimens, AT was an intramuscular tendon of GM, which exhibited a strap-like morphology that was proximodistally wide (Figs. 2, 3). In Sakura and Rimi, its proximodistal width was approximately 20mm and 25mm, respectively, and thickness was 3mm and 1mm, respectively. The AT was thus well-developed in Sakura whereas it was thinner but wider in Rimi. In both specimens, the AT attached along the inferolateral (anterior) margin of the LSP. Posterior to the attachment site, the AT wrapped around the LSP and the posterolateral femoral diaphysis such that it had contact with (but did not adhere to) the surface of the femoral diaphysis (Figs. 2B, 3A). GM and VL separated from each other proximally, whereas distally they seemed to insert into a common deep fascia continuous from the proximal LIM; thus both muscles attached along the posterolateral femoral diaphysis.

VL formed a thick tendinous origin on the greater trochanter in both specimens. In both specimens, the VL attached to the ILF by means of muscular fibers (Figs. 2C, 3C). The two specimens exhibited different connective tissue anatomies in the region of ILF. In Sakura, the lateral portion of the VL was perforated by tendinous fibers (of which the diameter was approximately 1-2mm) of GM. These fibers directly inserted into the ILF immediately distal to the AT attachment site (Fig. 2). The VL muscular portion and GM tendinous fibers appeared to cross each other (Fig. 2C). In contrast to Sakura, in Rimi, the ILF was the site of attachment of both VL muscular fibers and LIM. The latter was a sheet-like structure immediately distal to the attachment site of AT (Fig. 3). In Rimi, there were no GM tendinous fibers perforating VL, and GM and VL appeared separated by LIM.

Virtual dissection

In both specimens, CT images show that a fleshy portion of VL extends posteromedially beyond LSP, and that GM muscle mass is situated further medially (posterior to the femoral diaphysis) at the level of LSP (Fig. 4). In the transverse section through LSP and ILF, it appears that the attachment site of GM on the femoral diaphysis occurs posteromedial to LSP, as indicated by the position of the LIM (Fig. 4), as proposed by Morimoto et al. (2011b). The physical dissection, however, showed that the AT did not adhere to the posteromedial side of LSP, but was juxtaposed to this region of the diaphysis, as suggested by Suwa et al. (Suwa et al., 2012). The attachment site of the AT was therefore confirmed to be inferolateral to LSP.

In Sakura, there is a region of VL that exhibits higher X-ray density (attenuation) than the surrounding muscles at the level of ILF (Fig. 4A, circle). This region corresponds to the position of VL muscular portion that is perforated by the GM tendinous fibers. Posterior to this region, there is a deep fascia between GM and VL, which exhibits higher X-ray density than the muscles (Fig. 4A). The CT image of Rimi is overall similar to that of Sakura, but the LIM is more clearly visible in this specimen, such that GM and VL appear more clearly separated.

Osteological features

The two chimpanzee specimens examined in this study show considerable morphological differences in both their trochanters and femoral diaphysis (Figs. 1, 4, 5). While Sakura exhibits a more squared-shape trochanter morphology with comparatively clear ridges, Rimi exhibits a more rounded morphology with little ridge development (Figs. 1, 4, 5). While Sakura exhibits a distinct LSP and weakly expressed ILF (Figs. 1F, 5B), Rimi exhibits a similarly developed LSP and a more pronounced ILF (Figs. 1G, 5B). The ILF region of Sakura is thus more like a rugose surface than a fossa. There is also a difference in the degree of rugosity of the ILF region. While the rugosity is well-developed in Sakura, in Rimi, the ILF area exhibits a comparatively smoother surface (Fig. 5). Furthermore, in Sakura, the rugosity extends superiorly onto a part of the LSP, whereas, in Rimi, the LSP and rugose ILF surface do not overlap.

Morphometric mapping analysis (Fig. 6) captures overall differences of the surface morphology of the femoral diaphysis as well as the difference in the specific regions of LSP and ILF (Figs. 5). Morphometric mapping data confirm that the surface topography of the LSP-ILF complex is more

222 substantially expressed in Rimi than in Sakura (Figs. 5). Further variations of the ILF and LSP are shown
223 in Morimoto et al. (2011a) and Suwa et al. (2012).

224

225 **Discussion**

226 The femoral musculature of the two chimpanzee specimens examined in this study is overall consistent
227 with that described in previous studies (Crass, 1952, Sigmon, 1974, Uhlmann, 1968, Stern, 1972,
228 Swindler and Wood, 1982). The answers to the questions addressed in this study are as follows:

229 • *Is the attachment site of the ascending tendon (AT) of* gluteus maximus *(GM) superomedial or*
230 *inferolateral to lateral spiral pilaster (LSP)?*
231 The attachment site of AT on the femur appears consistently inferolateral to LSP. The attachment
232 site of AT has a more rugose surface than the LSP.
233 • *Is vastus lateralis (VL) attached on the inferolateral fossa (ILF)?*
234 VL is attached to the ILF by means of muscular fibers in both specimens examined in this study.
235 • *Where does the lateral intermuscular septum (LIM) attach relative to the lateral spiral pilaster*
236 *(LSP) and inferolateral fossa (ILF)?*
237 In one individual (Rimi), the LIM was a sheet-like tendinous structure at the level of LSP and ILF,
238 that attaches into the ILF. In the other individual (Sakura), LIM was not present as a sheet-like
239 structure at the ILF, but took the form of a deep fascia. The VL muscular portion at ILF was
240 perforated by the GM tendinous fibers, which inserted directly into the ILF.

241 These results are consistent with Lovejoy et al. (2002) (Fig. 1C) in that the attachment site of the
242 chimpanzee GM on the proximal femur is inferolateral to LSP, not posteromedial (Morimoto et al., 2011),
243 and that the LSP separates the insertion of the GM from the adductor origin. However, contrary to
244 Lovejoy et al. (2002), and in accordance with Morimoto et al. (2011b), the two specimens dissected here
245 indicate that the ILF serves as an attachment site for the VL muscular fibers and also for LIM (Fig. 1D).
246 Thus, the results of the present study corroborate Lovejoy et al's. (2002, 2009) description of the
247 topographic pattern of the chimpanzee femoropelvic muscles, in that the GM insertion occurs lateral to
248 the LSP to form a LSP-GM/VL medial to lateral relationship, as reviewed by Suwa et al. (2012). At the
249 same time, our results indicate that interpretations of the osseous morphology of the ILF by Suwa et al.
250 (2012) were incorrect, and that the chimpanzee ILF is probably best characterized as an area where the
251 fibrous attachments of both GM and VL contribute to its rugosity and morphology.

Furthermore, the results of this study indicate that CT-based virtual dissection data must be interpreted with care. First, it must be checked whether a muscle or its tendon is attached to a given bone, or whether it is merely juxtaposed to it (Suwa et al., 2012). To overcome this problem, for example, during CT data acquisition of fresh cadavers, a specimen can be scanned in different positions. It could then be checked whether the muscles move relative to each other and to the bone, or whether the muscle positions remain fixed in different scans. Second, the spatial and contrast resolutions of CT-based images must be considered as factors limiting identification of anatomical features of interest. For example, in one of the specimens examined in this study, the VL muscular portion was perforated by the GM tendinous fibers (Fig. 2C). In the CT images, however, the multiple sets of these tendinous GM fibers are indistinguishable from the muscular fibers of VL or from each other. Instead, the tendinous (GM) and muscular (GM+VL) portions appear as a single undifferentiated region of higher X-ray density (attenuation) (Fig. 4A). These problems could potentially be circumvented by using a contrast agent, which would improve the spatial and contrast resolutions of the CT images. It has been shown that such contrast agents, in combination with high-resolution micro-CT scans, successfully improve quality of CT images, and enable distinction of anatomical features at the level of fibrous structures (Cox and Jeffery, 2011, Jeffery et al., 2011). These latter authors examined the musculoskeletal morphology of rodent heads, which are suitable for micro-CT scans, but the methods used in these studies could in principle be applied to larger specimens such as great apes. Also, MRI (magnetic resonance imaging) of fresh cadavers would be an important complement to CT imaging.

In both specimens examined in this study, the ILF is an attachment site of the muscular fibers of VL. However, in addition to the VL, in one of the specimens, ILF serves as an attachment site for the tendinous fibers of GM, and in the other specimen a well-developed LIM attaches into the ILF. These patterns represent anatomical variation in the chimpanzee GM/VL interface that has not been described previously. These results indicate that the proximal femoral musculature potentially exhibits considerable variation, and that visually similar skeletal features may not necessarily correspond to identical connective tissue structures. In other words, the results of this study indicate that – within certain constraints – muscle attachment sites vary relative to bone surface morphology. Accordingly, inferring attachment sites from bone surface morphology needs to take such variation into account.

Variation of muscle structure and musculo-skeletal correspondence observed in this study leads to the question as to how the association of soft- and hard-tissue structures (GM, VL and ILF) can be generalized in chimpanzees. Our results indicate that, for the chimpanzee femoral diaphysis, a sensible interpretation would be that the ILF generally represents a boundary region of GM and VL rather than the attachment site of either muscle exclusive to the other (Fig. 1E). In this view, ILF can be interpreted as

the shared attachment site of GM and VL. This view would encompass the variation observed in this study, but it also raises new questions. An interesting question is how GM and VL relate to each other in terms of development. This question could also be generalized as follows: how does the continuum of connective tissue (fascia *sensu* (Schleip et al., 2012)) between muscles differentiate into histologically distinguishable structures during development? These questions are critical, since new structures arise only by the modification of developmental programs during the course of evolution. It is thus of special relevance to investigate developmental patterns, to the extent possible, both in living and fossil species. In this study, only adult individuals were examined, but studying the development of the femoropelvic musculature could provide further insights into the evolutionary modification of the femoropelvic structures in hominoids. For example, the human GM consists of a single segment in adults, but it consists of two segments early in the prenatal period (Tichý and Grim, 1985). The two segments originate from the sacroiliac region and coccyx, respectively, and fuse into a single GM during the later prenatal period (Tichý and Grim, 1985). In all great apes, GM consists of two portions, the proximal and distal portions (GM proprius [GMp] and ischiofemoralis [GMi]). In adults, GMp and GMi together form a single muscle in chimpanzees and gorillas, while they are separated from each other in orangutans (Sigmon, 1974). Currently, it is unknown whether GM in chimpanzees and gorillas arise from two segments during early ontogeny, and if so, when during ontogeny the fusion occurs and where in GM the border between the two segments lies. Answering these questions could help us understand whether apparent similarities of femoropelvic muscle structure between chimpanzees and gorillas come from common ancestry or from convergent evolution in each lineage. This is also of special relevance to understanding how taxon-specific developmental programs associated with femoropelvic musculature evolved in humans and chimpanzees from those of their last common ancestor.

This study adds to the knowledge of proximal femoral musculoskeletal topography of chimpanzees by means of combining real and virtual dissections. It shows that our knowledge of chimpanzees—our closest living relative —is still incomplete, even at the macroscopic anatomy level. On the one hand, it is important to recognize that even a limited part of the musculoskeletal system such as the lateral spiral pilaster and neighboring fossa holds evolutionary significance. On the other hand, evolutionary questions of great ape comparative anatomy could also be addressed from a wider perspective of primates, and it is beyond the scope of this study to discuss such evolutionary history of the hominoid femoropelvic muscle structure. At the same time, the discussion that arose between Morimoto et al. (2011b) and Suwa et al. (2012) has led to an alternative fruitful avenue of investigation. It is time to study bone-muscle correspondence in an extended sample of immature and adult great ape specimens. Combining the advantages of virtual and physical dissections will provide new insights on intra- and

318 interspecific variation of musculo-skeletal topography. Such data of the femoropelvic region will permit
319 reexamination of various evolutionary scenarios of hominid locomotion, for example as proposed by the
320 functional analysis of the proximal femora of the earliest hominids (Lovejoy et al., 2009a, Lovejoy et al.,
321 2009b, Senut et al., 2001, Pickford et al., 2002, Almécija et al., 2013).

Acknowledgements

We are grateful to Tobe Zoo, Tenoji Zoo, Higashiyama Zoom, the GAIN (Great Ape Information Network) project of Japan, and Primate Research Institute of Kyoto University, Japan (KUPRI) for data of Rimi and Sakura. We also thank anonymous reviewers for their valuable comments and suggestions.

References

Almécija S, Tallman M, Alba DM, Pina M, Moyà-Solà S, Jungers WL (2013) The femur of *Orrorin tugenensis* exhibits morphometric affinities with both Miocene apes and later hominins. *Nat Commun,* **4**.

Beddard F (1893) Contributions to the anatomy of the anthropoid apes. *Trans. Zool. Soc. London,* **13,** 177-218.

Bramble DM, Lieberman DE (2004) Endurance running and the evolution of *Homo*. *Nature,* **432,** 345-352.

Carrier DR, Anders C, Schilling N (2011) The musculoskeletal system of humans is not tuned to maximize the economy of locomotion. *Proc Natl Acad Sci U S A,* **108,** 18631-6.

Champneys F (1871) On the muscles and nerves of a chimpanzee (*Troglodytes niger*) and a *Cynocepalus anubis*. *J. Anat. Lond.,* **6,** 176-211.

Cox PG, Jeffery N (2011) Reviewing the morphology of the jaw-closing musculature in squirrels, rats, and guinea pigs with contrast-enhanced microCT. *The Anatomical Record: Advances in Integrative Anatomy and Evolutionary Biology,* **294,** 915-928.

Crass E (1952) Musculature of the hip and thigh of the chimpanzee : a comparison to man and other primates. *PhD thesis, Univ. Wisconsin*.

Hepburn D (1892) Comparative anatomy of the muscles and nerves of the superior and inferior extremities of the anthropoid apes: Part II. *J Anat Physiol,* **26,** 324-56.

Jeffery NS, Stephenson RS, Gallagher JA, Jarvis JC, Cox PG (2011) Micro-computed tomography with iodine staining resolves the arrangement of muscle fibres. *Journal of Biomechanics,* **44,** 189-192.

Lieberman DE, Raichlen DA, Pontzer H, Bramble DM, Cutright-Smith E (2006) The human gluteus maximus and its role in running. *Journal of Experimental Biology,* **209,** 2143-2155.

Lovejoy CO (2005) The natural history of human gait and posture: Part 1. Spine and pelvis. *Gait & Posture,* **21,** 95-112.

Lovejoy CO, Meindl RS, Ohman JC, Heiple KG, White TD (2002) The Maka femur and its bearing on the antiquity of human walking: Applying contemporary concepts of morphogenesis to the human fossil record. *American Journal of Physical Anthropology,* **119,** 97-133.

Lovejoy CO, Suwa G, Simpson SW, Matternes JH, White TD (2009a) The great divides: *Ardipithecus ramidus* reveals the postcrania of our last common ancestors with African apes. *Science,* **326,** 100-106.

Lovejoy CO, Suwa G, Spurlock L, Asfaw B, White TD (2009b) The pelvis and femur of *Ardipithecus ramidus*: The emergence of upright walking. *Science,* **326,** 71.

Marzke MW, Longhill JM, Rasmussen SA (1988) Gluteus maximus muscle function and the origin of hominid bipedality. *American Journal of Physical Anthropology,* **77,** 519-28.

Morimoto N, Zollikofer CPE, Ponce de León MS (2011a) Exploring femoral diaphyseal shape variation in wild and captive chimpanzees by means of morphometric mapping: a test of Wolff's Law. *Anatomical Record,* **294,** 589-609.

Morimoto N, Zollikofer CPE, Ponce de León MS (2011b) Femoral morphology and femoropelvic musculoskeletal anatomy of humans and great apes: a comparative virtopsy study. *Anatomical Record,* **294,** 1433-1445.

368 Pickford M, Senut B, Gommery D, Treil J (2002) Bipedalism in *Orrorin tugenensis* revealed by its
369 femora. *Comptes Rendus Palevol,* **1,** 191-203.
370 Primrose A (1898) The anatomy of the Orang utang (*Simia satyrus*). *Trans. Canad. Inst.,* **6,** 507-598.
371 Raven H (1950) Regional anatomy of the gorilla. In *The Anatomy of the Gorilla* (ed Gregory W). New
372 York: Columbia University Press.
373 Schleip R, Jäger H, Klingler W (2012) What is 'fascia'? A review of different nomenclatures. *Journal of*
374 *Bodywork and Movement Therapies,* **16,** 496-502.
375 Senut B, Pickford M, Gommery D, Mein P, Cheboi K, Coppens Y (2001) First hominid from the
376 Miocene (Lukeino Formation, Kenya). *C. R. Acad. Sci. Paris Ser. II a,* **332,** 137-144.
377 Sigmon BA (1974) A functional analysis of pongid hip and thigh musculature. *Journal of Human*
378 *Evolution,* **3,** 161-185.
379 Stern JT (1972) Anatomical and functional specializations of human gluteus maximus. *American Journal*
380 *of Physical Anthropology,* **36,** 315-338.
381 Stern JT, Susman RL (1981) Electromyography of the gluteal muscles in *Hylobates*, *Pongo*, and *Pan* -
382 implications for the evolution of hominid bipedality. *American Journal of Physical Anthropology,*
383 **55,** 153-166.
384 Suwa G, Lovejoy CO, Asfaw B, White T (2012) Proximal femoral musculoskeletal morphology of
385 chimpanzees and its evolutionary significance: a critique of Morimoto et al. (2011). *The*
386 *Anatomical Record: Advances in Integrative Anatomy and Evolutionary Biology***,** n/a-n/a.
387 Swindler D, Wood C (1982) *An Atlas of Primate Gross Anatomy,* Robert E. Krieger Publishing Company,
388 Malabar.
389 Thali MJ, Dirnhofer R, Vock P (2009) The Virtopsy Approach.). New York: CRC Press.
390 Thali MJ, Jackowski C, Oesterhelweg L, Ross SG, Dirnhofer R (2007) Virtopsy - The Swiss virtual
391 autopsy approach. *Legal Medicine,* **9,** 100-104.
392 Thorpe SK, Crompton RH, Gunther MM, Ker RF, McNeill Alexander R (1999) Dimensions and moment
393 arms of the hind- and forelimb muscles of common chimpanzees (*Pan troglodytes*). *American*
394 *Journal of Physical Anthropology,* **110,** 179-99.
395 Tichý M, Grim M (1985) Morphogenesis of the human gluteus maximus muscle arising from two muscle
396 primordia. *Anat Embryol (Berl),* **173,** 275-7.
397 Uhlmann K (1968) Hüft- und Oberschenkelmuskulatur: Systematische und vergleichende Anatomie. In
398 *Primatologia: Handbuch der Primatenkunde* (eds Hofer H, Schultz AH, Starck D). Basel: Karger.
399 Voronov AV (2003) Anatomical cross-sectional areas and volumes of the muscles of the lower
400 extremities. *Human Physiology,* **29,** 201-211.

401 **Figure legends**

402 Fig. 1 Proximal femoral morphology and muscle attachment sites in chimpanzees. A: bone morphology
403 of the posterolateral femoral diaphysis. B: bone surface topography. Muscle attachment areas are depicted
404 as proposed by Lovejoy et al. (2002) and Suwa et al. (2012) (C), and by Morimoto et al. (2011) (D). E:
405 consensus view of muscle attachment areas observed in this study. VL does not have a fibrous attachment
406 on the femoral diaphysis in the region between its trochanteric origin and ILF. F-G: proximal femoral
407 morphology and corresponding muscle attachment areas in the specimens examined in this study. SMF:
408 superomedial fossa. AT: Ascending tendon. GM: *gluteus maximus*. ILF: inferolateral fossa. LIM: lateral
409 intermuscular septum. LSP: lateral spiral pilaster. VL and VI: *vastus lateralis* and *vastus intermedius*.

410

411 Fig. 2 Proximal musculature of right femur in Sakura. A: AT is an intramuscular tendon of GM. B: the
412 attachment site of AT is inferolateral to LSP, while AD inserts superomedially to the LSP. C: boundary
413 region of GM and VL (after fixation by formaldehyde solution). VL is attached to the ILF by means of
414 muscular fibers. VL is perforated by the tendinous fibers of GM, which inserts into the ILF distal to the
415 attachment site of AT. LSP: lateral spiral pilaster. ILF: inferolateral fossa. AD: adductor muscle. AT:
416 ascending tendon of *gluteus maximus*. BF: *biceps femoris*. GM: *gluteus maximus*. VL and VI: *vastus*
417 *lateralis* and *vastus intermedius*.

418

419 Fig. 3 Proximal musculature of right femur in Rimi. A: AT is a thin strap-like tendon. B: the attachment
420 site of AT is inferolateral to LSP. Blue arrowheads indicate the attachment site of the tendon of adductor
421 muscle, superomedial to the LSP. C: boundary region of GM and VL. VL is attached to the ILF by means
422 of muscular fibers. D: GM and VL are separated by LIM at the level of ILF. VL attaches to the ILF. LSP:
423 lateral spiral pilaster. ILF: inferolateral fossa. LIM: lateral intermuscular septum. AD: adductor muscle.
424 AT: ascending tendon of *gluteus maximus*. BF: *biceps femoris*. GM: *gluteus maximus*. VL and VI: *vastus*
425 *lateralis* and *vastus intermedius*.

426

427 Fig. 4 Cross-sectional CT image at the level of lateral spiral pilaster (LSP) and inferolateral fossa (ILF),
428 and bone surface rendering of the proximal femur. A: Sakura. B: Rimi. Arrowheads indicate the lateral
429 spiral pilaster.

430

431 Fig. 5 Proximal femoral morphology and areas of muscle attachment sites. A: Sakura. B: Rimi. AD:
432 adductor muscle. Yellow arrowheads indicate the positions of cutmarks marked by the surgical knife in
433 the physical dissection; blue arrowheads indicate position of AD insertion; red lines indicate the course of
434 the ascending tendon (AT). GM: *gluteus maximus*. ILF: inferolateral fossa. LSP: lateral spiral pilaster.
435 LIM: Lateral intermuscular septum. Scale bar = 2 cm.

436

Fig. 6 Morphometric mapping of the surface morphology of the femoral diaphysis. The surface topography is visualized along the entire length of the femoral diaphysis in Sakura (A) and Rimi (B). The false-color scale indicates the local radius of curvature (relative units; data are normalized to their respective median values); fossae appear in dark blue, and ridges in red. ILF: white arrowheads point to inferolateral fossa, LSP: black arrowheads point to lateral spiral pilaster. LA: linea aspera.

442 Table 1. List of specimens

Specimen ID	Reference ID in this study	Individual age	Sex	Body weight at death (kg)
TPZ/TZ-Sakura	Sakura	39 y	F	-
PRISK-8828 (HZB-Rimi)	Rimi	>20y	F	24

443

Abbreviations

AD: adductor muscle

AT: ascending tendon

GM: *gluteus maximus*

ILF: inferolateral fossa

LIM: lateral intermuscular septum

LSP: lateral spiral pilaster

SMF: superomedial fossa

VL: *vastus lateralis*

VI: *vastus intermedius*

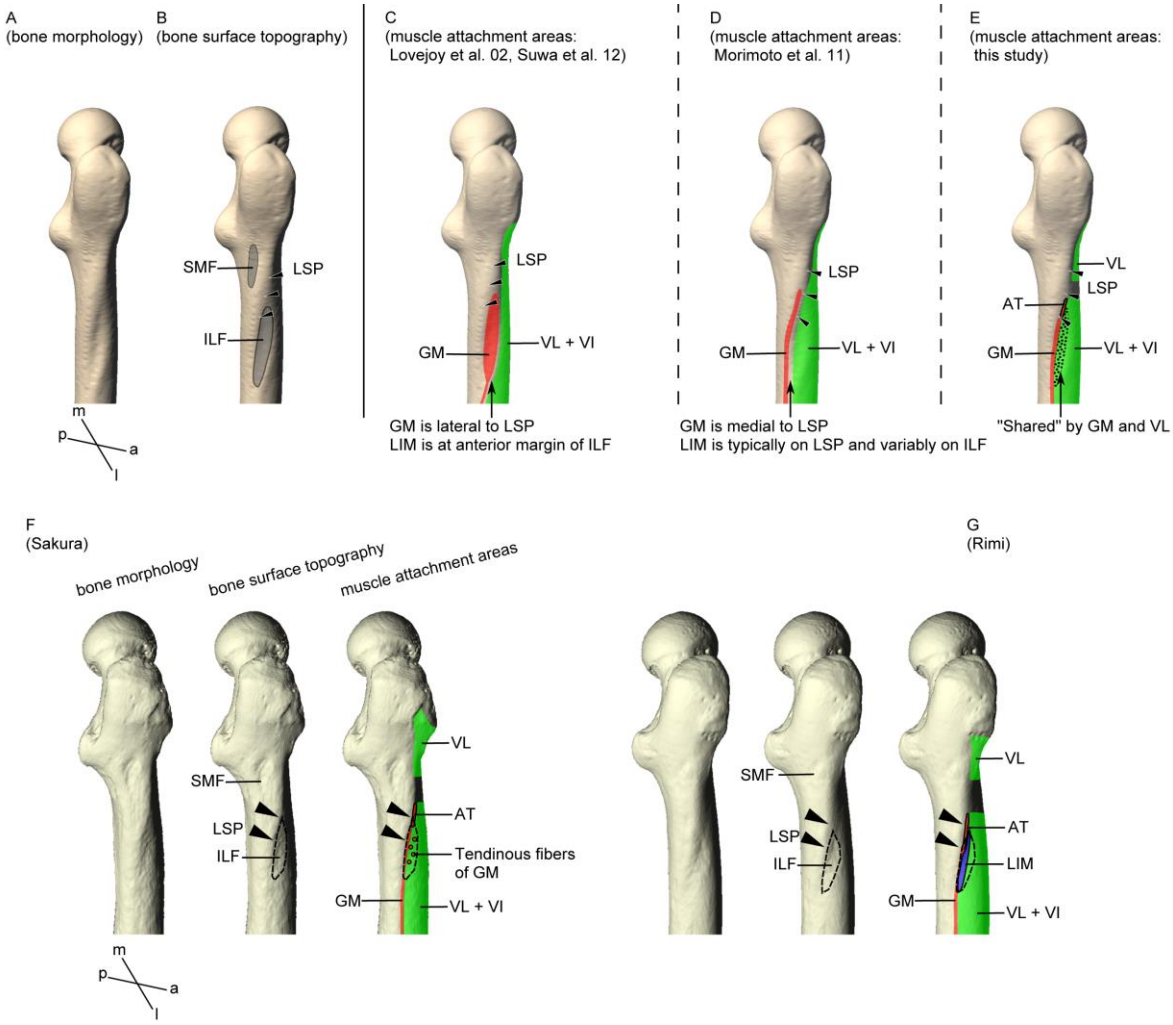
A
(bone morphology)
B
(bone surface topography)
C
(muscle attachment areas:
Lovejoy et al. 02, Suwa et al. 12)
D
(muscle attachment areas:
Morimoto et al. 11)
E
(muscle attachment areas:
this study)
SMF
LSP
ILF
m
p
a
l
LSP
GM
VL + VI
GM is lateral to LSP
LIM is at anterior margin of ILF
LSP
GM
VL + VI
GM is medial to LSP
LIM is typically on LSP and variably on ILF
VL
LSP
AT
GM
VL + VI
"Shared" by GM and VL
F
(Sakura)
bone morphology
bone surface topography
muscle attachment areas
SMF
LSP
ILF
VL
AT
Tendinous fibers
of GM
GM
VL + VI
m
p
a
l
G
(Rimi)
SMF
LSP
ILF
VL
AT
LIM
GM
VL + VI

454

455 Fig. 1

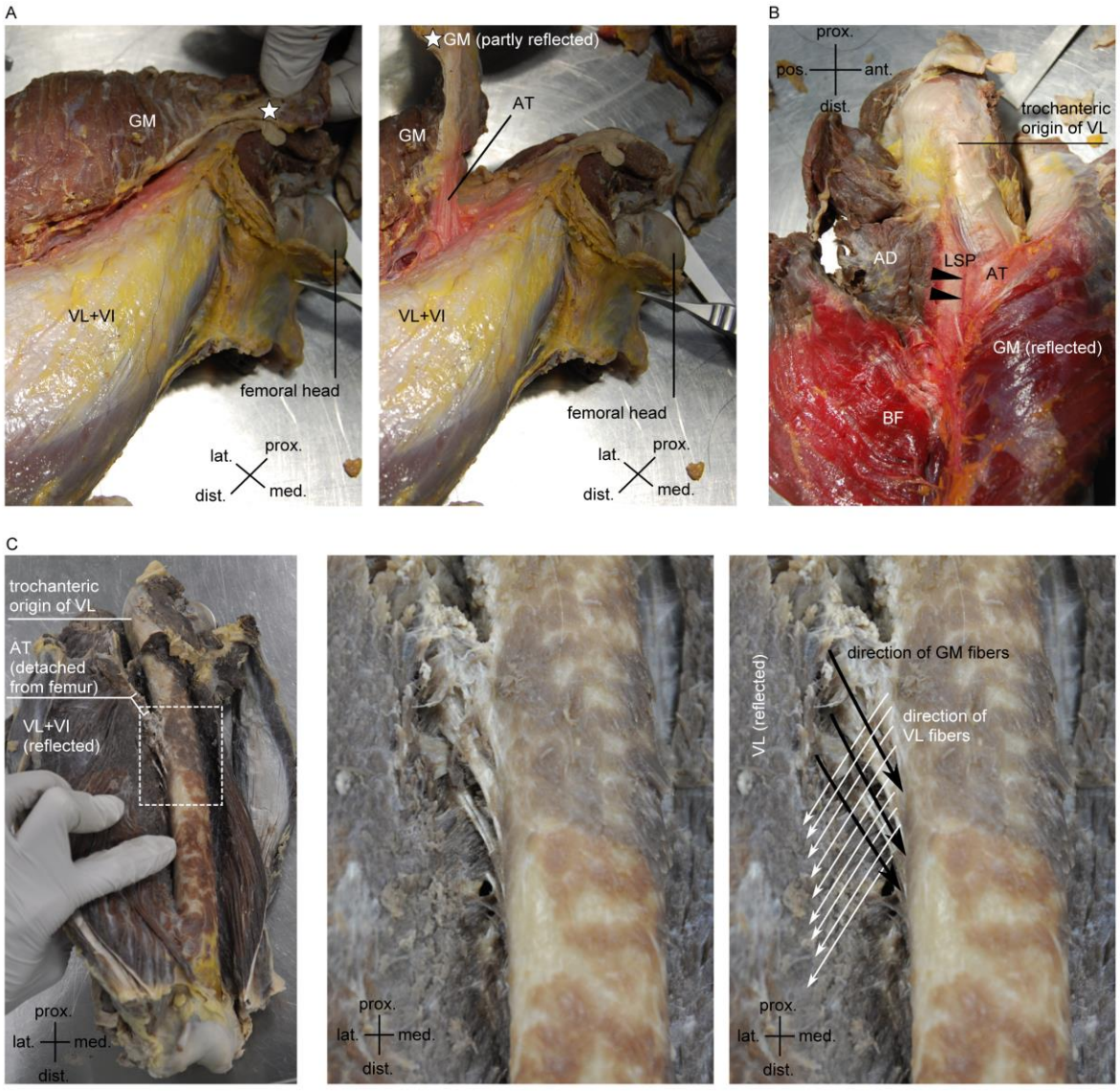
A
GM
VL+VI
femoral head
lat.
prox.
dist.
med.
GM (partly reflected)
AT
GM
VL+VI
femoral head
lat.
prox.
dist.
med.
B
prox.
pos.
ant.
dist.
trochanteric origin of VL
AD
LSP
AT
GM (reflected)
BF
C
trochanteric origin of VL
AT (detached from femur)
VL+VI (reflected)
prox.
lat.
med.
dist.
prox.
lat.
med.
dist.
direction of GM fibers
direction of VL fibers
VL (reflected)
prox.
lat.
med.
dist.

456

457 Fig. 2

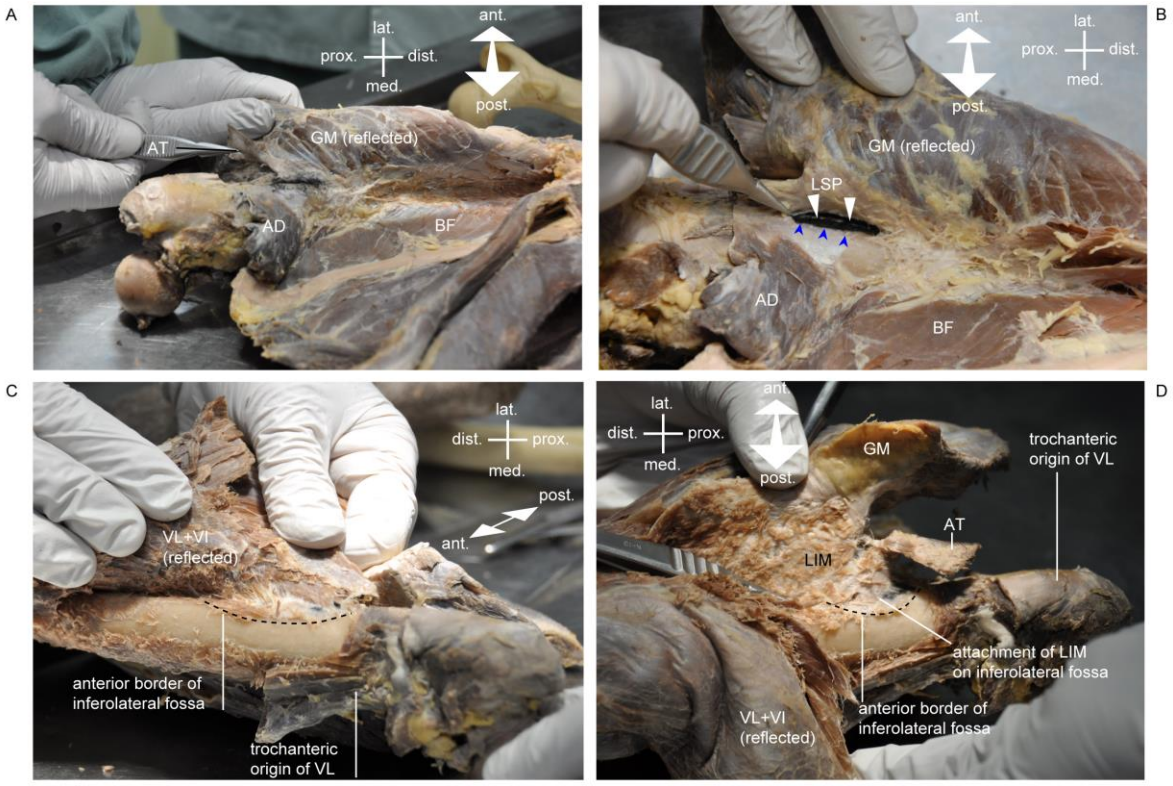
A
lat.
prox.
dist.
med.
ant.
post.
AT
GM (reflected)
AD
BF
B
ant.
lat.
prox.
dist.
med.
post.
GM (reflected)
LSP
AD
BF
C
lat.
dist.
prox.
med.
post.
ant.
VL+VI
(reflected)
anterior border of
inferolateral fossa
trochanteric
origin of VL
D
lat.
dist.
prox.
med.
ant.
post.
GM
trochanteric
origin of VL
AT
LIM
attachment of LIM
on inferolateral fossa
VL+VI
(reflected)
anterior border of
inferolateral fossa

458

459 Fig. 3

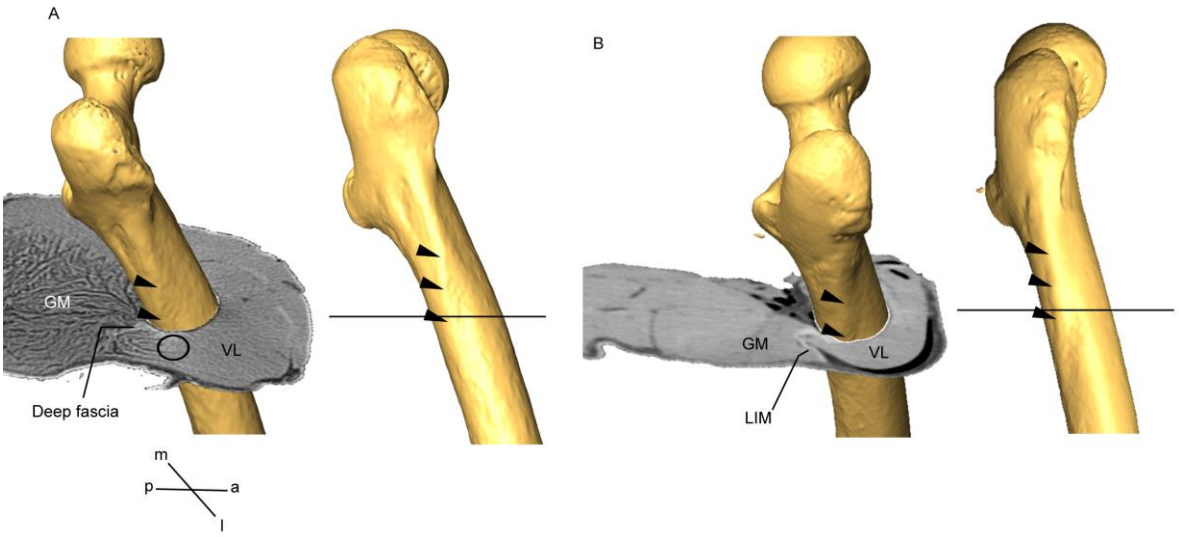

460

461 Fig. 4

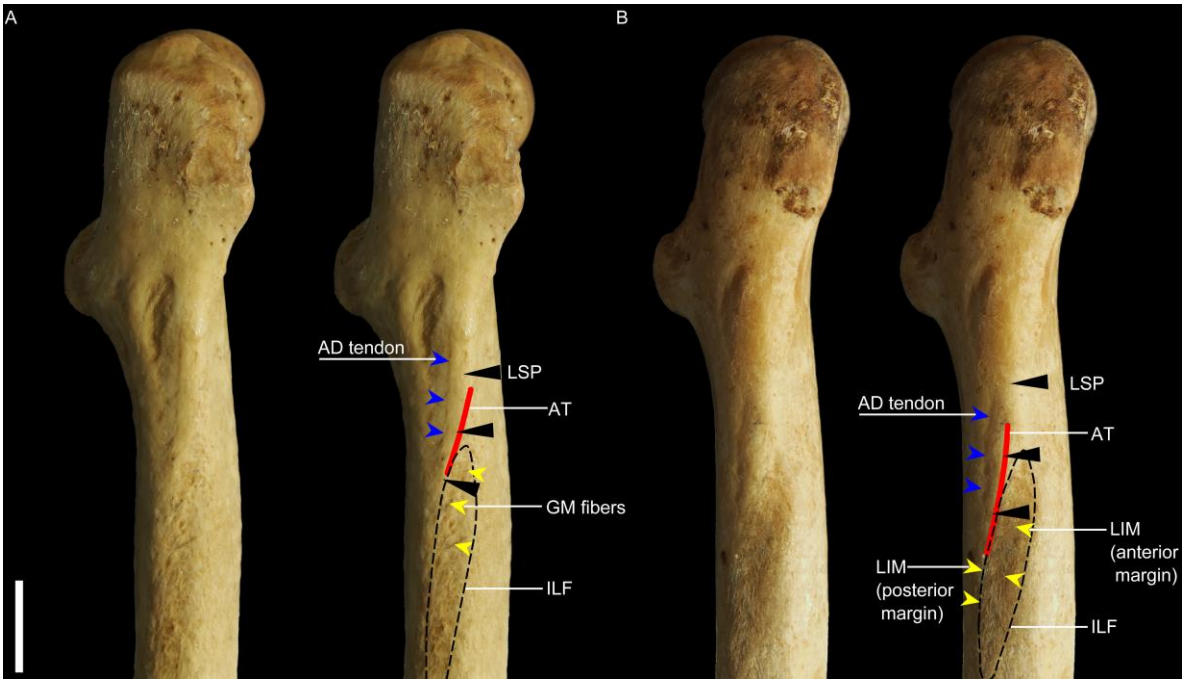
A
AD tendon
LSP
AT
GM fibers
ILF
B
AD tendon
LSP
AT
LIM
(anterior
margin)
LIM
(posterior
margin)
ILF

462

463 Fig. 5

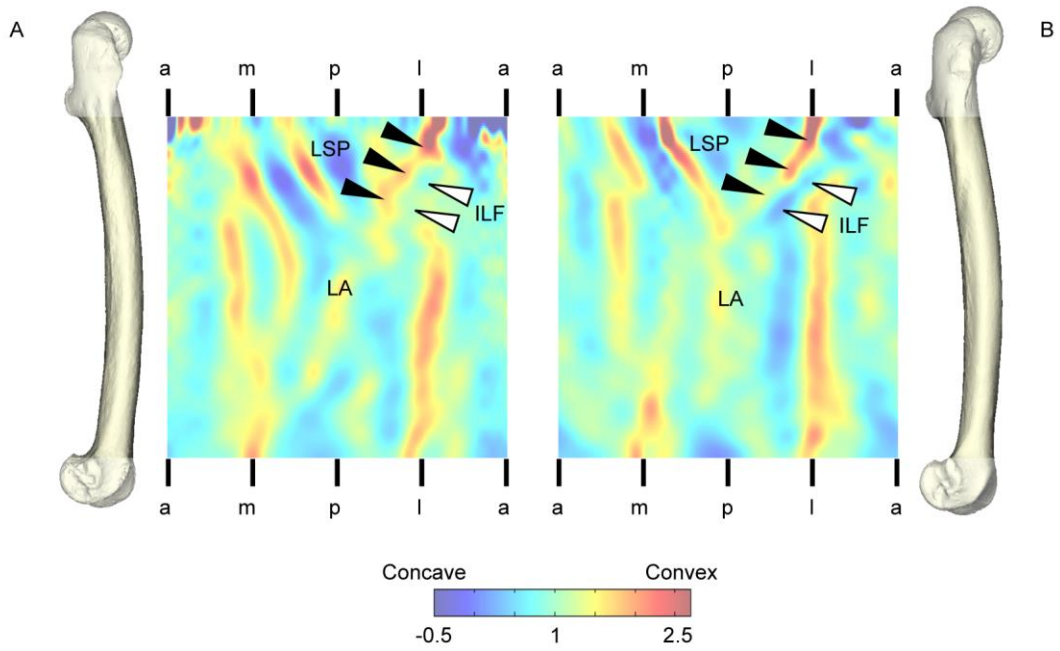
A
B
a m p l a
a m p l a
LSP
ILF
LA
LSP
ILF
LA
a m p l a
a m p l a
Concave
Convex
-0.5
1
2.5

464

465 Fig. 6